Journal of Alloys and Compounds 509 (2011) 4420–4425

Contents lists available at ScienceDirect

Journal of Alloys and Compounds

journal homepage: www.elsevier.com/locate/jallcom

Directional solidification and microstructural development of $Al_2O_3/GdAlO_3$ eutectic ceramic *in situ* composite under rapid growth conditions

Haijun Su*, Jun Zhang, Jianzheng Yu, Lin Liu, Hengzhi Fu

State Key Laboratory of Solidification Processing, Northwestern Polytechnical University, Xi'an 710072, PR China

ARTICLE INFO

Article history:
Received 24 October 2010
Received in revised form 17 January 2011
Accepted 18 January 2011
Available online 22 January 2011

Keywords:
Directional solidification
Al2O3/GdAlO3
Eutectic ceramics
Microstructure

ABSTRACT

Oxide eutectic ceramic *in situ* composites prepared by directional solidification from the melt in the Al_2O_3–Ln_2O_3 systems are promising candidates for the manufacture of turbine blades because of their excellent mechanical properties. With high temperature gradient and rapid cooling rate, directionally solidified (DS) $Al_2O_3/GdAlO_3$(GAP) eutectic ceramics having smooth surface and full density are successfully prepared by laser zone remelting at the scanning rate of 240–720 mm/h. The microstructure development and solidification behaviour under rapid growth rate are investigated. Fine typical DS irregular eutectic structure of "Chinese script" consisting of interpenetrating α-Al_2O_3 and GAP phases is obtained at the scanning rate below 360 mm/h. Further increasing the scanning rate, the as-solidified Al_2O_3/GAP eutectic presents a combination of "Chinese script" and elongated colony microstructure with complex regular structure. Inside the colonies, the rod-type or lamellar-type eutectic microstructures with ultra-fine GAP surrounded by the Al_2O_3 matrix are observed. The interphase spacing is strongly dependent on the laser scanning rate, rapidly decreasing to the sub-micron range for the samples grown at the highest rate. Moreover, the formation condition and solidification mechanism of the particular microstructure of the ceramic composite during rapid solidification are discussed.

1. Introduction

In the area of turbo-engines for aerospace and stationary power generation, there is a continuous demand for new ultra-high temperature structural materials with high strength and thermal stability at elevated temperatures, and consequently, improving the energy efficiency and reducing the polluting emission such as CO_2 and NOx [1–3]. It is well known that eutectic *in situ* composite ceramics have high melting point, hardness, creep resistance and sufficient chemical stability at elevated temperatures but are sensitive to plastic deformation [4,5]. Eutectic oxide composites produced by directional solidification, in which the eutectic phases are generated simultaneously from the melt, possess very high structural stability and superior mechanical strength at high temperatures compared to individual components [6,7], and there is free of porosity in them in comparison with sintered ceramics [8]. Especially, eutectic *in situ* composites are composed of single crystal phases with a huge amount of clean interfaces between them, effectively eliminating grain boundaries and amorphous phases at interface [9–11]. Typical interphase spacing is generally in the micrometer range [12]. Therefore, over recent decades, directionally solidified (DS) oxide eutectic ceramic *in situ* composites have attracted the most attention because of outstanding properties derived from their unique microstructures: excellent high strength almost constant from room temperature to close to the melting point, good creep and oxidation resistance, superior microstructural stability (~1800 °C) and no chemical reaction between the constituent phases [13–16]. The unique characteristics render these composites more advantageous than single crystals or sintered ceramic composites [17]. Thus, theses materials are considered to be of great potentiality as new type of structural materials for stable use in an oxidizing atmosphere at temperatures higher than 1650 °C, allowing to be applied in gas turbine and power generation blades without cooling protection at high temperatures [18]. Furthermore, the unique microstructures of regular eutectics, made up of ordered arrays of alternating lamellae or fibres, are also promising candidates for use in several functional applications, such as optical, electronic, magnetic and in the energy production [12,19–21].

Among a series of DS Al_2O_3-based eutectic ceramics, the recently-developed $Al_2O_3/GdAlO_3$(GAP) eutectic *in situ* composite ceramic stands out due to its excellent high temperature strength retention and relative good toughness [13]. The eutectic composite has a new microstructure, in which a continuous network of single-crystal Al_2O_3 phase and single-crystal GAP phase interpenetrates without grain boundaries. The interlocked microstructure results in very high strength. Particularly, the Al_2O_3/GAP eutectic composite exhibits a flexural strength of about 700 MPa from

* Corresponding author. Tel.: +86 29 88492228; fax: +86 29 88494080.
E-mail address: shjnpu@yahoo.com.cn (H. Su).

0925-8388/$ – see front matter © 2011 Elsevier B.V. All rights reserved.
doi:10.1016/j.jallcom.2011.01.107

room temperature to 1600 °C, which is almost two times of that of the $Al_2O_3/Y_3Al_5O_{12}$ eutectic ceramic. The toughness of the composite can reach 5–6 MPa·$m^{1/2}$, which is almost two times of that of the $Al_2O_3/Y_3Al_5O_{12}$ eutectic ceramic [13,22,23]. The hollow non-cooling turbine nozzle vane prepared from the Al_2O_3/GAP eutectic ceramic has been recently reported [15], and the thermal efficiency predicted can be improved 9% [24]. However, due to the very high melting point (>1700 °C) and processing difficulties, the preparation of Al_2O_3/GAP eutectic ceramic by conventional directional solidification method is very difficult and the cost is very high. Using the laser heated pedestal growth technique, the Al_2O_3/GAP eutectic fiber has been obtained by Andreeta et al. [25], but the eutectic growth is limited to a low rate and the volume is very small. Consequently, the experimental data and solidification mechanism for Al_2O_3/GAP eutectics are still limited and often uncertain [26]. Furthermore, the solidification microstructure plays a key role in determining eutectic growth mechanism and consequent mechanical properties [27]. Most of previous studies on DS Al_2O_3/GAP eutectic rods are primarily used by the Bridgman method [13,22,24] or were focused on low growth rate [22–26]. Nevertheless, the temperature gradient of Bridgman method is very low (<100 K/cm), which leads to low growth rate and large interphase spacing (>10 μm). Thus the understanding and control of solidification microstructure in theory and practice are insufficient, and further improvement in mechanical properties is extremely restricted. In order to refine the solidification microstructure, higher thermal gradients (>10^3 K/cm) and consequently a smaller interphase spacing (<1 μm) can be expected to attain by using zone meting methods [16,28,29]. Laser zone remelting is recently developed directional solidification technique for preparing oxide eutectic composite with advantages of no need of crucible, very high melting temperature, large thermal temperature gradient (>10^4 K/cm) and high growth rates [30–32], but is few applied to Al_2O_3/GAP eutectic ceramics yet. One additional advantage over the floating zone method is the possibility of producing large areas of DS eutectics. With the laser zone remelting technique, the aims of the present paper are to prepare the DS Al_2O_3/GAP eutectic ceramic *in situ* composite under high temperature gradient, and to investigate solidification process and microstructure development at rapid growth conditions.

2. Experimental details

The eutectic rods and plates of $Al_2O_3/GdAlO_3$ were prepared by the laser zone remelting technique according to the following process. Commercially available high purity (>4 N) nano-powders of Al_2O_3 and Gd_2O_3 were used as starting materials. The two powders were homogenously mixed with 10vol% polyvinyl alcohol in an agate mortar in the eutectic mole ratio of Al_2O_3/Gd_2O_3 = 77/23 according to the phase diagram, as shown in Fig. 1 [33]. The Ø7 mm × 80 mm precursor rods and 10 mm × 70 mm × 5 mm plates were prepared by die pressing for 10 min at 25 MPa and pressureless sintering for 2 h at 1500 °C. The final sintered specimens had densities around 70% of the theoretical density. Laser zone remelting was carried out with a 5 kW continuous wave CO_2 laser (Rofin-Sinar 850) in a vacuum environment (10^{-2} Pa). The laser beam was focused to a spot with the diameter of 4 mm. The power density was used from 16 to 40 W/mm^2 and the scanning velocities varied from 240 to 720 mm/h. The sample was moved by the numerically-controlled worktable with 5-axis and 4-direction coupled motion to realize the laser beam scanning along the sample axis. Under the strong radiation of the high energy laser, the sample was rapidly remelted and directionally solidified just behind the melting zone alone the *X* direction, as illustrated in Fig. 2a. The laser was unmoved. The melted zone spanned the width of the sample surface, and the whole or the surface of the precursor could be resolidified. In order to avoid volatilization and reduce pores during solidification, the high purity Ar gas was filled into the vacuum chamber at the flow rate of 10 L/min.

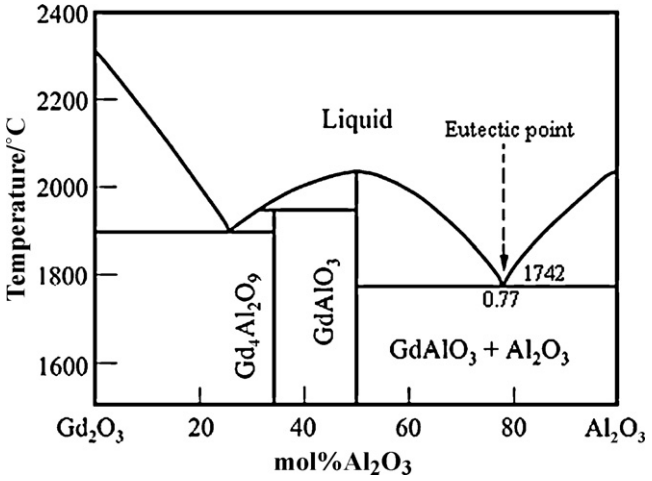

Fig. 1. Phase diagram of the Al_2O_3–Gd_2O_3 binary oxide system.

Transverse and longitudinal cross-sections of the as-solidified samples were cut and treated with the conventional metallographic technique. The polished sample surface was etched in the H_3PO_4 solution at 70 °C. The microstructures were observed using scanning electron microscope (SEM, SUPRA-55). The phases and components of the composite were characterized by energy dispersive spectroscopy (EDS, LINK-ISIS), and X-ray diffractometer (XRD, RIGAKUMSG-158). Quantitative calculation of the phase volume fraction and interphase spacing were performed by digital image analysis software of SISC IAS V8.0.

3. Results and discussion

During laser zone remelting, the precursor density, laser power and scanning rate play important roles on the sample quality and the relationships between processing variables and final microstructure characteristic. In our experiment, it is found that the 70% precursor density is suitable value to apply in the laser zone remelting. Higher density can easily lead to fracture and cracks between the solidified layer and the remaining non-melted zone.

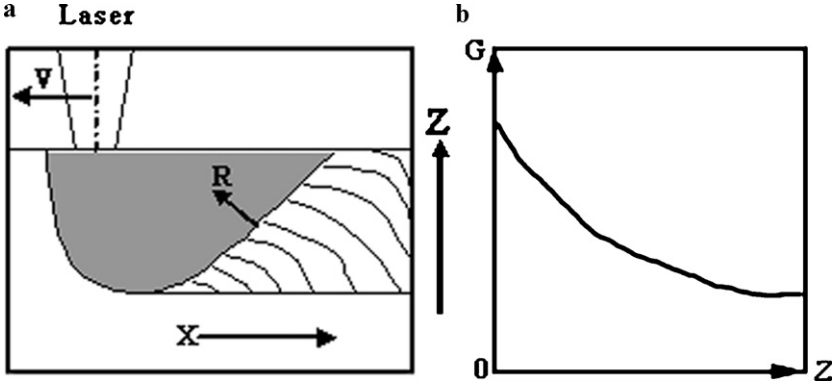

Fig. 2. Schematics of the laser zone remelting processing (a) and the change of temperate gradient G with the distance Z from the bottom to top of the solidified layer (b). *V* is the scanning rate, *R* is the solidification rate, and *X* is the scanning direction.

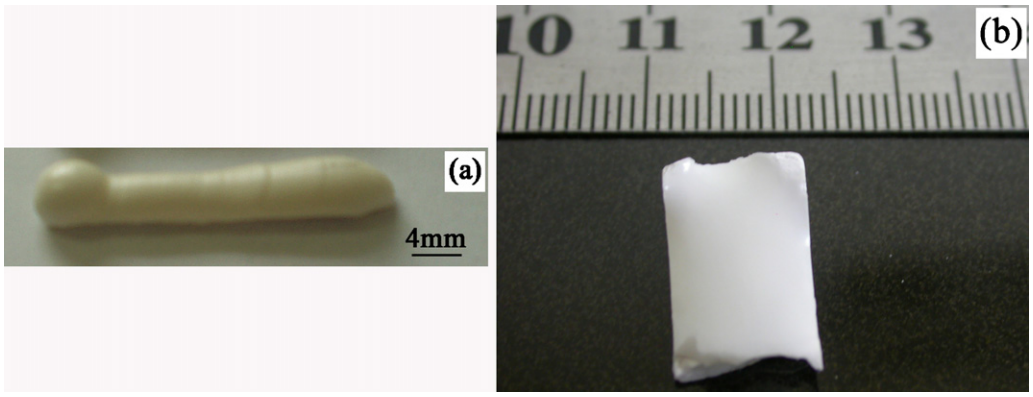

Fig. 3. Photographs of laser remelted Al_2O_3/GAP eutectic ceramic rod (a) and plate (b).

Moreover, the elimination of the cracks due to rapid cooling or residual stress and gas porosity introduced during the melting process are the key of influencing the ceramic melt preparation [34]. Specially, the thermal residual stresses produced during cooling due to mismatch of thermal expansion coefficients of the eutectic phases often cause sample cracking, importantly affecting the forming quality. Compared to the Al_2O_3–ZrO_2 eutectic with large thermal residual stresses (>1 GPa) [35,36], the GAP and Al_2O_3 phases in the Al_2O_3-GAP eutectic have similar thermal expansion efficiencies of about $8.0 \times 10^{-6}\,K^{-1}$, so very small thermal residual stresses can be produced, which is similar to the Al_2O_3-YAG eutectic [37]. In order to reduce the thermal stress, one of the effective ways is to preheat the processing zone or the substrate. Using the backheating method, Gurauskis et al. [38] prepared the dense crack-free Al_2O_3–ZrO_2 plates with large areas by laser-assisted surface remelting. The processing parameters are varied to find the optimum parameters to prepare the Al_2O_3/$GdAlO_3$ eutectic ceramics in order to obtain sufficient remelting/solidification and to reduce or suppress surface defects such as cracks and pores. In the present study, we use the laser of 500–1000 W to preheat the substrate to high temperature about 800 °C, and then start the ceramic remelting. It is found that the fracture and crack formed during solidification are obviously reduced. Furthermore, by inputting the non-oxidant gas of Ar from both the top and bottom of the substrate, the porosity and gas inclusion are effectively avoided. Because the laser absorptivity of oxides is beyond 60% [39], only small power density is enough to remelt the sintered precursor. Considerable experimental results show that the continuous-wave output CO_2 laser operated at 190–500 W with a scanning rate of 240–720 mm/h successfully melts the Al_2O_3–Gd_2O_3 samples, producing solidified rods or plates with smooth surface and high density, as shown in Fig. 3. The Al_2O_3/GAP eutectic rods have diameters about 4–6 mm (Fig. 3a) and the plates have thickness about 0.1–2 mm (Fig. 3b) depended on the laser processing parameters.

The typical microstructure of the transverse cross-section of the as-solidified Al_2O_3/GAP eutectic grown at the scanning rate of 360 mm/h is shown in Fig. 4a. For comparison, the microstructure of the sintered precursor with same composition is given in Fig. 4b. The SEM analysis indicates that the laser remelted Al_2O_3/GAP eutectic presents a very fine "Chinese script" pattern consisting of α-Al_2O_3 phase with a corundum structure and GAP phase with a perovskite structure without any other phases between them determined by XRD and EDS. No pores and cracks are observable in the microstructure. Similar microstructure has also been observed previously in other Al_2O_3-based eutectic ceramics, such as Al_2O_3-YAG [13,26], and Al_2O_3-EAG [40]. Because of the relatively rapid growth rate compared to general directional solidification, the cellular microstructure is also observed, as shown by the black arrows in Fig. 4a. The gray area is GAP phase and the dark area is Al_2O_3 phase. In contrary, for the sintered composite with same composition (Fig. 4b), the microstructure displays a coarse polycrystalline ceramic structure with clear pores and grain boundaries, which reveals that laser zone remelting effectively improves the composite microstructure. SEM image analysis indicates the volume fraction of GAP phase is about 0.52, which favorably agrees with that expected for eutectic composition.As is well known, the selection of phases and their patterns during solidification generally depends on alloy composition and solidification conditions. For laser zone remelting, the microstructure evolution of oxide eutectic is manly dependent on the laser scanning rate due to few volatilizations of oxides and no contamination in the preparation process [32]. The liquid-solid interface morphology is curved and changes with the melt zone depth. The growth direction varies from perpendicular to the bottom to parallel to the top of the solidified surface, which leads to a variable temperature gradient with the melting zone depth, as illustrated in Fig. 2b. The highest growth rate happens at the solidification layer surface. Fig. 5 shows the transverse cross-section microstructure of the Al_2O_3/GAP eutectic ceramics grown at the further increased scanning rates. The composite presents an inclined growth array along the scanning direction. On the contrary, the microstructure of the longitudinal cross-section of the as-solidified sample (Fig. 6) shows a directional growth array along the scanning direction as usually occurs in DS metal eutectics [41], which results from the solidification direction nearly parallel to the free surface and the highest solidification rate. The interphase spacing increases towards the inner of the solidified layer. Overall, the microstructure orientation is parallel to the precursor transfer direction (X direction in Fig. 2a). Additionally, because the laser zone remelting has very high temperature gradient of 10^4–10^5 K/cm [32], the coupled eutectic growth can also be retained even at high growth rate. The interphase spacing analysis is chosen at the region near to the sample surface. As the laser scanning increases, the interphase spacing is rapidly decreased. The average interphase spacing is only 0.1–1.2 μm when the rate is at 720 mm/h, which is almost 1/10 of that of the Al_2O_3/GAP eutectic prepared availably by Bridgman method [22]. The obtainment of ultra-fine eutectic microstructure is primarily attributed to rapid solidification rate and high temperature gradient during laser zone remelting process. Moreover, in comparison with typical regular eutectic morphology [42], the Al_2O_3/GAP eutectic composite presents a complex irregular lamellar structure, which primary results from the high volume fraction of eutectic phases (>1/π) and the high entropies of fusion of oxides leading to strong faceted growth interface [3,17]. However, in comparison with the Al_2O_3/YAG eutectic [10], the tendency to form facets in Al_2O_3/GAP is relatively weak. Fiber distribution with a greater relative quantity

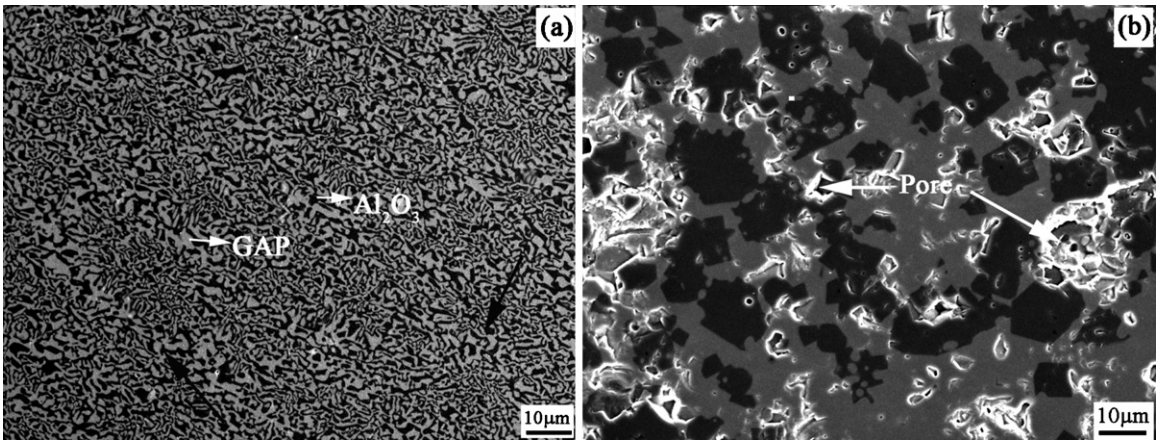

Fig. 4. SEM images of transverse sections showing the typical microstructural comparison of the as-solidified Al_2O_3/GAP eutectic ceramic composite grown at the scanning rate of 360 mm/h (a) and the sintered sample (b) with the same composition.

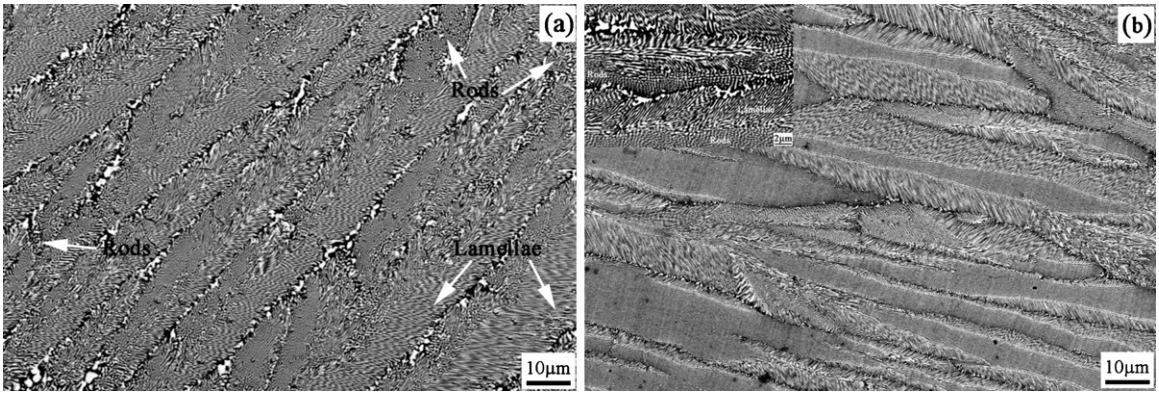

Fig. 5. SEM images of the transverse cross-section microstructure of the laser remelted Al_2O_3/GAP eutectic sample grown at various scanning rates: (a) 480 mm/h and (b) 720 mm/h. The inset is the magnification of (b). The samples were cut perpendicular to the laser scanning direction.

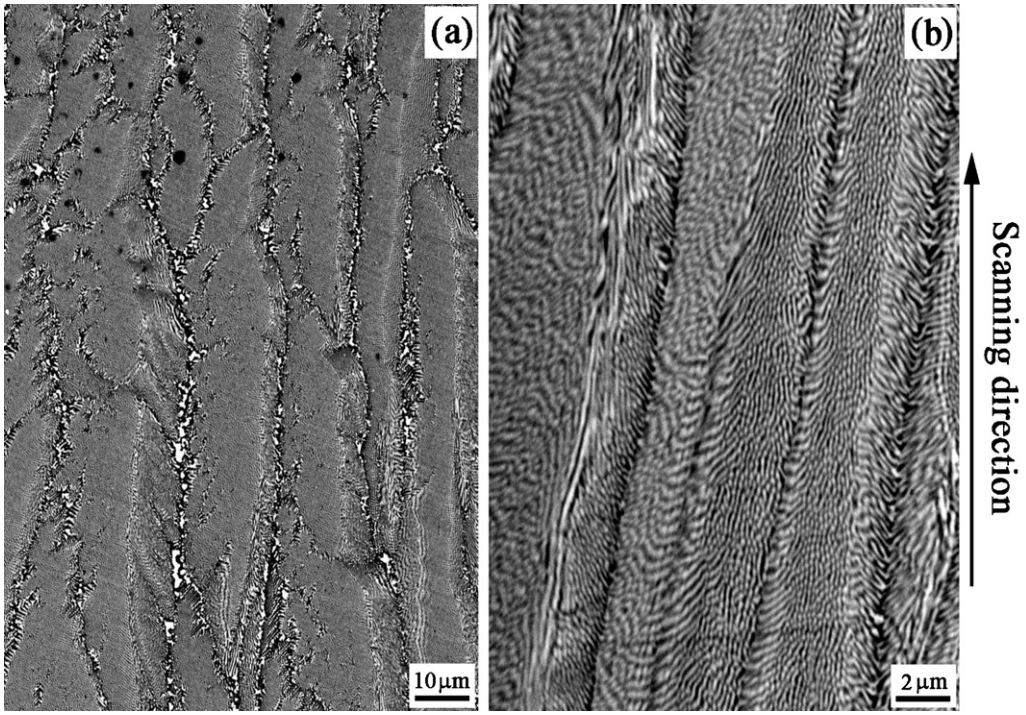

Fig. 6. SEM images showing the longitudinal microstructure of the laser remelted Al_2O_3/GAP eutectic sample grown at different scanning rates: (a) 480 mm/h and (b) 720 mm/h.

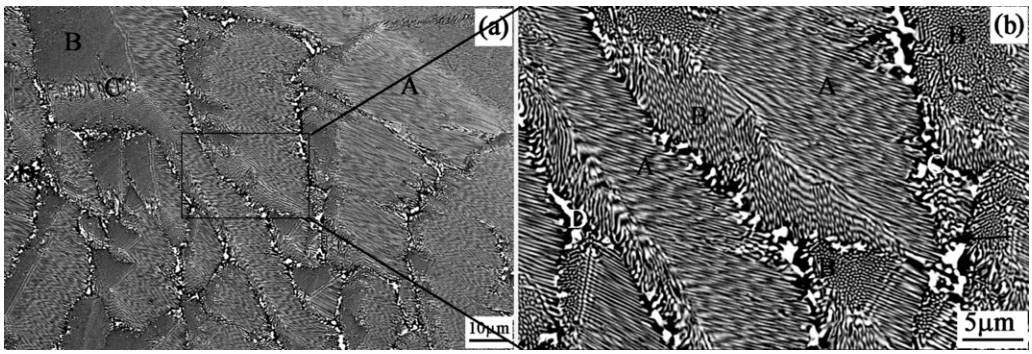

Fig. 7. SEM images showing the heterogeneous microstructure appeared in the laser remelted Al_2O_3/GAP eutectic grown at 720 mm/h (a) and the detail (b) of the four different microstructure types formed (A - lamellae; B - rods; C - Chinese script; D - cellular).

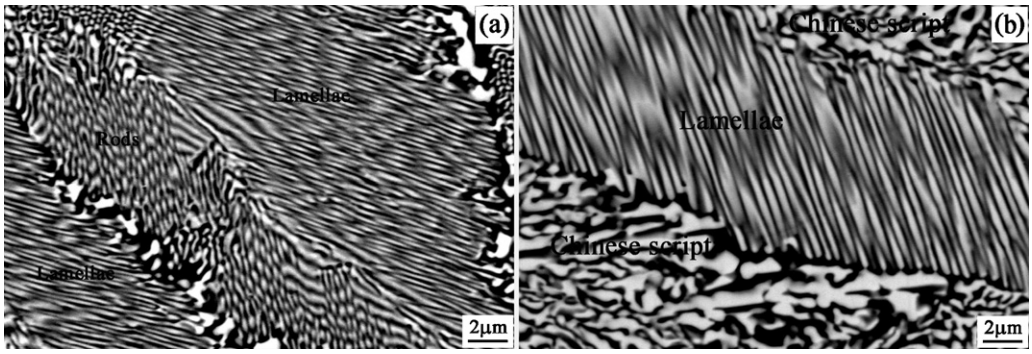

Fig. 8. SEM images showing the transition of lamellae to rods (a) and the transition of Chinese script to lamellae in the laser remelted Al_2O_3/GAP eutectic composite (b).

of complex regular regions tends to produce at high growth rates (Figs. 5b and 6). The observed microstructure with the particular features in the eutectic apparently satisfies Jackson's criterion [43].

Furthermore, as compared with Fig. 4a, an increase of laser scanning rate causes the formation of a colony structure (Figs. 5 and 6). The size of colony is about 5–10 μm and decreases with increasing the laser scanning rate. In the colony, the complex-regular rod-like or lamellar structure is observed, as shown by the arrows in Fig. 5a and the magnification of Fig. 5b. Similar phenomena are also observed by Medeiros et al. [26] in the DS Al_2O_3/GAP eutectic prepared by laser heated pedestal growth and the LaB_6–ZrB_2 ceramic eutectic at high growth rate [44], but is few reported in previous other binary oxide eutectic system without dopant [15,45] even if at the same growth conditions. For instance, in the Al_2O_3-YAG binary eutectic, the microstructure presents homogenous morphology even at high growth rate [46], differently to the Al_2O_3/GAP eutectic. The same development to form colonies was also observed by Sayir and Farmer [6] in the Y_2O_3 doped Al_2O_3/ZrO_2 eutectic. Pastor et al. [47] found the microstructure of the Al_2O_3/ZrO_2 (Y_2O_3) eutectic transformed from homogenous irregular eutectics to colonies with thick intercolony region and to elongated cells with thin intercellular boundaries as the growth rate increased. Ester et al. [48] reported that the onset of the colony formation in the Al_2O_3/YAG/YSZ ternary eutectic was produced at the scanning rate of 500 mm/h. Because no composition change is observed in the present study, this further reveals the Al_2O_3/GAP eutectic tends to grow in more regular morphology as the solidification rate is raised. The formation of the colony is mainly caused by the interface perturbations and the constitutional undercooling taken at the curved solid-liquid front under rapid solidification rate. Furthermore, it is found that the Al_2O_3/GAP eutectic grown at the scanning rate of 720 mm/h appears a non-homogeneous microstructure, in which four different morphology regions (A: lamellae; B: rods; C: Chinese script; D: cellular) can be classed, as shown in Fig. 7a. The magnified image of the four regions is shown in Fig. 7b. This indicates that a coexistence of "Chinese script" structure and complex regular structure favors to appear in the Al_2O_3/GAP eutectic, especially at high growth rates. From this point, the Al_2O_3/GAP eutectic may be considered to tend to grow as a faceted/non-faceted behavior [49] different with the Al_2O_3/YAG eutectic although all the eutectic phases have high entropies of fusion [17]. The eutectic growth is determined not only by the physical properties of materials but also by the growth conditions [50]. Thus there is necessarily a transition between the irregular and regular morphology during the Al_2O_3/GAP eutectic growth. In our case, the transition of lamellae to rods and the transition of Chinese script to lamellae in the eutectic are shown in Fig. 8a and b, respectively. During crystal growth, the growth of faceted eutectic is general unstable [18], in which the faceted phase may transit into the weakly faceted phase or non-faceted phase under rapid solidification. As a result, the transition of irregular Chinese script to complex regular eutectic structures is produced during the non-equilibrium solidification process of the laser zone remelting.

4. Conclusions

Laser zone remelting has been successfully applied to prepare bulk densified Al_2O_3/GAP eutectic *in situ* composite ceramics free of macroscopic defects such as pores and cracks. The microstructure development under high growth rate range is investigated. The as-solidified eutectic composite shows a very fine "Chinese script" structure at low scanning rate and elongated colony structure consisting of only α-Al_2O_3 and GAP phases without grain boundaries, pores and amorphous phase at high scanning rate. In the colony, the complex-regular rod and lamellae structure are observed. With increasing the laser scanning rate, the lamellar spacing rapidly decreases. The average interphase spacing is about 0.1–1.2 μm at the rate of 720 mm/h. The transition of irregular "Chinese script" to

complex-regular rod-like or lamellar structure is verified experimentally, which are primarily attributed to the transition of faceted to non-faceted growth of eutectic phases and the non-equilibrium solidification processing during laser zone remelting under rapid growth conditions.

Acknowledgments

Thanks are given to the National Natural Science Foundation of China (51002122, 50772090), the Provincial Natural Science Foundation of Shaanxi Province (2010JQ6005), the Aeronautical Science Foundation of China (2010ZF53064), the NPU Foundation for Fundamental Research (NPU-FFR-G9KY1016), the Opening Project of State Key Laboratory for Advanced Metals and Materials (2007AMM004), the research fund of the State Key Laboratory of Solidification Processing in NWPU (76-QP-2011), the 111 Project (B08040), the Scientific Research Start-up Foundation of NPU (GAKY3006), and the New People and New Directions Foundation of School of Materials Science and Engineering in NPU (09XE0104-5).

References

[1] S. Gopagoni, J.Y. Hwang, A.R.P. Singh, B.A. Mensah, N. Bunce, J. Tiley, T.W. Scharf, R. Banerjee, J. Alloys Compd. 509 (2011) 1255–1260.
[2] T. Zhang, W.L. Ren, J.W. Dong, X. Li, Z.M. Ren, G.H. Cao, Y.B. Zhong, K.Z. Deng, S. Lei, J.T. Guo, J. Alloys Compd. 487 (2009) 612–617.
[3] I. Bogomol, T. Nishimura, O. Vasylkiv, Y. Sakka, P. Loboda, J. Alloys Compd. 505 (2010) 130–134.
[4] Y. Waku, N. Nakagawa, H. Ohtsubo, A. Mitani, K. Shimizu, J. Mater. Sci. 36 (2001) 1585–1594.
[5] I. Bogomol, O. Vasylkiv, Y. Sakka, P. Loboda, J. Alloys Compd. 490 (2010) 557–561.
[6] A. Sayir, S.C. Farmer, Acta Mater. 48 (2000) 4691–4697.
[7] H. Kaiden, S.D. Durbin, A. Yoshikawa, J.H. Lee, K. Sugiyama, T. Fukuda, J. Alloys Compd. 336 (2002) 259–264.
[8] J.M. Ma, F. Ye, L.M. Liu, H.J. Zhang, J. Alloys Compd. 493 (2010) L15–L18.
[9] C.T. Rios, A.A. Coelho, W.W. Batista, M.C. Gonçalves, R. Caram, J. Alloys Compd. 472 (2009) 65–70.
[10] Y. Waku, T. Sakuma, J. Eur. Ceram. Soc. 20 (2000) 1453–1458.
[11] I. Bogomol, T. Nishimura, O. Vasylkiv, Y. Sakka, P. Loboda, J. Alloys Compd. 485 (2009) 677–681.
[12] R.I. Merino, J.I. Peña, A. Larrea, G.F. de la Fuente, V.M. Orera, Recent Res. Dev. Mat. Sci. 4 (2003) 1–24.
[13] Y. Waku, N. Nakagawa, T. Wakamoto, H. Ohtsubo, K. Shimizu, Y. Kohtoku, Nature 389 (1997) 49–52.
[14] J. Martinez Fernandez, A. Sayir, S.C. Farmer, Acta Mater. 51 (2003) 1705–1720.
[15] J. Llorca, V.M. Orera, Prog. Mater. Sci. 51 (2006) 711–809.
[16] P.B. Oliete, J.I. Peña, A. Larrea, V.M. Orera, J. Llorca, J.Y. Pastor, A. Martin, J. Segurado, Adv. Mater. 19 (2007) 2313–2318.
[17] H.J. Su, J. Zhang, C.J. Cui, L. Liu, H.Z. Fu, J. Cryst. Growth 307 (2007) 448–456.
[18] H.J. Su, J. Zhang, Y.F. Deng, L. Liu, H.Z. Fu, Scripta Mater. 60 (2009) 362–365.
[19] J.I. Peña, R.I. Merino, G.F. de la Fuente, V.M. Orera, Adv. Mater. 8 (1996) 909–912.
[20] M. Kruczek, E. Talik, D.A. Pawlak, K. Kołodziejak, T. Łukasiewicz, J. Alloys Compd. 442 (2007) 255–258.
[21] L. Ortega-San-Martin, J.I. Peña, A. Larrea, V. Gil, V.M. Orera, Int. J. Hydrogen Energy 35 (2010) 11499–11504.
[22] Y. Waku, Adv. Mater. 10 (1998) 615–617.
[23] S. Ochiai, T. Ueda, K. Sato, M. Hojo, Y. Waku, N. Nakagawa, S. Sakata, A. Mitani, T. Takahashi, Comp. Sci. Technol. 61 (2001) 2117–2128.
[24] N. Nakagawa, H. Ohtsubo, A. Mitani, K. Shimizu, Y. Waku, J. Eur. Ceram. Soc. 25 (2005) 1251–1257.
[25] E.R.M. Andreeta, M.R.B. Andreeta, A.C. Hernandes, J. Cryst. Growth 234 (2002) 782–785.
[26] I.S. Medeiros, E.R.M. Andreeta, A.C. Hernandes, J. Mater. Sci. 42 (2007) 3874–3877.
[27] J.G. Fan, X.Z. Li, Y.Q. Su, J.J. Guo, H.Z. Fu, J. Alloys Compd. 506 (2010) 593–599.
[28] H.J. Su, J. Zhang, Y.F. Deng, L. Liu, H.Z. Fu, J. Alloys Compd. 456 (2008) 518–523.
[29] N. Sekido, Y. Kimura, S. Miura, F. Wei, Y. Mishima, J. Alloys Compd. 425 (2006) 223–229.
[30] A. Larrea, G.F. de la Fuente, R.I. Merino, V.M. Orera, J. Eur. Ceram. Soc. 22 (2002) 191–198.
[31] P. Gargarella, R. Vilar, A. Almeida, C.S. Kiminami, C.T. Rios, C. Bolfarini, W.J. Botta, J. Alloys Compd. 495 (2010) 646–649.
[32] H.J. Su, J. Zhang, L. Liu, H.Z. Fu, Comp. Sci. Technol. 69 (2009) 2657–2667.
[33] Y.H. Han, M. Nagata, N. Uekawa, K. Kakegawa, Br. Ceram. Trans. 103 (2004) 219–222.
[34] P.B. Oliete, J.I. Peña, J. Cryst. Growth 304 (2007) 514–519.
[35] V.M. Orera, R.I. Merino, J.A. Pardo, A. Larrea, J.I. Peña, C. González, P. Poza, J.Y. Pastor, J. Llorca, Acta Mater. 48 (2000) 4683–4689.
[36] N.R. Harlan, R.I. Merino, J.I. Peña, A. Larrea, V.M. Orera, C. González, P. Poza, J. Llorca, J. Am. Ceram. Soc. 85 (2002) 2025–2032.
[37] J.Y. Pastor, J. LLorca, A. Salazar, P.B. Oliete, I. de Francisco, J.I. Peña, J. Am. Ceram. Soc. 88 (2005) 1488–1495.
[38] J. Gurauskis, V. Lennikov, G.F. de la Fuente, R.I. Merino, J. Eur. Ceram. Soc. (2010), doi:10.1016/j.jeurceramsoc.2010.08.017.
[39] H.J. Su, J. Zhang, J.J. Tian, L. Liu, H.Z. Fu, J. Appl. Phys. 104 (2008) 023511–23517.
[40] N. Nakagawa, H. Ohtsubo, Y. Waku, H. Yugami, J. Eur. Ceram. Soc. 25 (2005) 1285–1291.
[41] E. Çadırlı, H. Kaya, M. Gündüz, J. Alloys Compd. 431 (2007) 171–179.
[42] A.T. Dutra, P.L. Ferrandini, C.A.R. Costa, M.C. Gonçalves, R. Caram, J. Alloys Compd. 399 (2005) 202–207.
[43] K.A. Jackson, J.D. Hunt, Trans. AIME 236 (1966) 1129–1142.
[44] C.M. Chen, L.T. Zhang, W.C. Zhou, J. Cryst. Growth 191 (1998) 873–878.
[45] J. Ramírez-Rico, A.R. Pinto-Gómez, J. Martínez-Fernández, A.R. de Arellano-López, P.B. Oliete, J.I. Peña, V.M. Orera, Acta Mater. 54 (2006) 3107–3116.
[46] J.Y. Pastor, J. Llorca, A. Martín, J.I. Peña, P.B. Oliete, J. Eur. Ceram. Soc. 28 (2008) 2345–2351.
[47] J.Y. Pastor, J. Llorca, P. Poza, I. de Francisco, R.I. Merinob, J.I. Peña, J. Eur. Ceram. Soc. 25 (2005) 1215–1223.
[48] J. Ester, A. Larrea, R.I. Merino, J. Eur. Ceram. Soc. (2010), doi:10.1016/j.jeurceramso c.2010.08.016.
[49] W.J. Yao, N. Wang, J. Alloys Compd. 487 (2009) 354–357.
[50] P. Ferrandini, W.W. Batista, R. Caram, J. Alloys Compd. 381 (2004) 91–98.